crystals

MDPI

Review

Review of Creep-Thermomechanical Fatigue Behavior of Austenitic Stainless Steel

Jingwei Zhao, Feng Qiu and Chuangang Xu *

Tianjin Jinhang Technical Physics Institute, Tianjin 300308, China
* Correspondence: 18920198283@189.cn

Abstract: Research on the creep-thermomechanical fatigue (CTMF) behaviors of austenitic stainless steel for nuclear power plant pipelines is reviewed in the present paper. The stress response behavior, the main damage mechanisms, including thermomechanical fatigue, creep, oxidation, and dynamic strain aging (DSA), as well as the effects of strain dwell type, dwell time, and temperature-strain phase angle on fatigue life behavior of austenitic stainless steel under CTMF loading conditions are systematically discussed, and the coupled effects of various damage mechanisms are revealed. It is emphasized that CTMF is closer to the actual service condition of nuclear power plant pipes. It is pointed out that the traditional method of life design based on the isothermal fatigue test data is not conservative. Finally, the research on CTMF behaviors of austenitic stainless steel for nuclear power plant is summarized and prospected.

Keywords: austenitic stainless steel; creep-fatigue; creep-thermomechanical fatigue; damage mechanism

check for updates

Citation: Zhao, J.; Qiu, F.; Xu, C. Review of Creep-Thermomechanical Fatigue Behavior of Austenitic Stainless Steel. *Crystals* **2023**, *13*, 70. https://doi.org/10.3390/cryst13010070

Academic Editor: Pavel Lukáč

Received: 30 November 2022
Revised: 19 December 2022
Accepted: 22 December 2022
Published: 1 January 2023

Copyright: © 2023 by the authors. Licensee MDPI, Basel, Switzerland. This article is an open access article distributed under the terms and conditions of the Creative Commons Attribution (CC BY) license (https://creativecommons.org/licenses/by/4.0/).

1. Introduction

Austenitic stainless steel is widely utilized as the main structural material for pipelines in pressurized water reactor (PWR) nuclear power plants, attributed to its excellent combination of mechanical properties at high temperatures and corrosion resistance. Compared with the third-generation PWR nuclear power plants, the operation temperature of the fourth-generation fast breeder reactor represented by the sodium-cooled fast reactor (SFR) is increased, with a maximum temperature of approximately 550 °C, which leads to the service conditions being more complicated. In addition, in order to achieve economic competitiveness, generally the design life of SFR is extended to 60 years at least, which is a severe test for the nuclear-grade structural materials [1,2]. Nuclear power pipes are subjected to cyclic mechanical loadings caused by internal pressure fluctuations, coupled with strain cycles due to start-up/shut-down or thermal transients. Accordingly, thermomechanical fatigue (TMF) failure has become one of the main limited factors for the service life of nuclear power pipelines [3–10]. In addition, during the long-term servicing conditions under elevated temperatures and pressures, mechanical loads and dead weight lead to the accumulation of creep damage. The interaction of creep and TMF, i.e., creep-thermomechanical fatigue (CTMF), causes the deformation behaviors and failure mechanisms to be more complicated [7–14]. In the laboratory, the introduction of dwell time at constant strain in the isothermal fatigue (IF) test, namely creep-fatigue interaction (CFI), is utilized to simulate the high-temperature service conditions. However, the method cannot take into account the coupled effects of temperature cycling and other damage mechanisms.

In addition, life behavior of components under actual service conditions is predicted based on the method of independent linear accumulation of creep and fatigue damage [15,16]. Nevertheless, numerous studies have shown that the damage accumulation rate under CFI loading conditions is much higher than the sum of damage accumulation rate under the individual action of fatigue and creep mechanisms [11,17]. Traditionally, the damage

assessment and life behavior of components under TMF loading conditions are predicted based on the data generated by IF testing [18]. However, nonconservative results are usually yielded in TMF tests due to the low thermal conductivity combined with a high coefficient of thermal expansion of austenitic stainless steel, which leads to a high thermal stress within pipelines, as well as the synergistic interaction of more activated damage mechanisms [19,20].

2. Methods

In the present paper, the research on the CTMF behaviors of austenitic stainless steel for nuclear power plants published during the last 50 years is reviewed systematically, and the differences between CFI and CTMF are discussed. Based on the existing studies, various damage mechanisms under CTMF loading conditions were analyzed, including TMF, creep, oxidation, and dynamic strain aging. Before writing the present work, the author utilized keywords of austenitic stainless steel, fatigue, creep-fatigue, and creep-thermomechanical fatigue to search relative studies, which were from ScienceDirect. Firstly, a rough reading of the studies was conducted, mainly focusing on the differences between CFI and CTMF, the interaction of damage mechanisms, and the effects of various factors on the CTMF life behavior. Then, after a screening of all studies, it was essential to read the selected works in detail, during which the contents of different parts were summarized and the results and discussions were compared. As a result, the present work mainly focuses on the interpretation of various damage mechanisms and qualitative analysis of effects of various factors on the CTMF life behavior, and discusses the future research direction of CTMF.

3. Stress Response Behavior under CTMF Loading Conditions

3.1. Cyclic Stress Response

Compared with TMF loading conditions, the introduction of strain dwell changes the cyclic stress response behavior, and the influence is more significant under the condition of low strain amplitudes or long dwell time [21,22]. Specifically, the introduction of strain dwell has no significant effect on the mean stress [7], but can attenuate and accelerate the cyclic hardening and prolong the cyclic softening process [15]. This can be attributed to a series of factors as follows: (1) the reduction of bearing area caused by intergranular cracks due to creep damage [15], (2) decreased action frequency of mobile dislocation pinning caused by the coarsening and growth of carbides [7], (3) decreased resistance to cyclic deformation due to the annihilation of dislocations and formation of substructures with low internal energy [15,23], and (4) softening effect caused by creep deformation [19]. In addition, Sauzay et al. [24] studied the CFI behaviors of austenitic stainless steel at various temperatures and found that the thermal recovery process led to the vanishing of dislocation dipoles, which decreased the intragranular back stress and attenuated the cyclic hardening. Sarkar et al. [20] presented that the dislocation-twin interaction during thermal recovery process and shear stress in the surface grains caused by creep deformation could allow the twin boundaries to locally annihilate and convert into single dislocation lines [20,25,26]. However, Sauzay et al. [24] found that there was a critical dwell time for the influence of strain dwell on the cyclic hardening behavior. When the dwell time was shorter than the critical value, the hardening effect caused by the interaction of dislocation–dislocation and dislocation–precipitate was stronger, which enhanced the cyclic hardening [2]. However, with the increase of dwell time, the softening effect of thermal recovery process became stronger [7,19], which attenuated the cyclic hardening gradually. Moreover, the critical dwell time was temperature dependent, and was shorter at high temperatures.

3.2. Stress Relaxation Behavior

Stress relaxation refers to the phenomenon that the strain amplitude remains constant while the stress gradually decreases during the hold period, as illustrated schematically in Figure 1a. In addition, Figure 1b,c, which originated from ref. [9], show the stress relaxation behavior in the stress-strain hysteresis loop at the half-life cycle and tensile

strain dwell, respectively. Generally, the stress relaxation process is divided into two stages: the initial fast relaxation and subsequent stable relaxation stages [15]. However, Reddy et al. [2] presented that the stress relaxation behavior was related to the dwell time. When the dwell time was long, the stress relaxation was found to show an irregular pattern consisting of plateaus, waviness, and gradual/rapid changes. During the hold period, thermal recovery process promotes the dislocation annihilation by the cross-slip of screw dislocations and climb of edge dislocations, as well as viscoplastic flow [22,25], thus leading to the occurrence of stress relaxation [27]. In the process of stress relaxation, the elastic strain transforms to inelastic strain with the gradual decrease of inelastic strain rate [11,19]. Generally, the creep damage is characterized quantitatively by the amount of stress relaxation at the half-life cycle, thus predicting the fatigue life. However, numerous studies [4,21] have reported a considerable stress relaxation at high strain amplitudes while a strong reduction in fatigue life is obtained at low strain amplitudes, which implies that the absolute magnitude of relaxed stress alone cannot be associated with the creep damage. Therefore, based on the creep damage mechanisms, Hales [12] proposed that the inelastic strain rate was more suitable to characterize creep damage. The inelastic strain rate higher than 10^{-4} s^{-1} during the stress relaxation contributes less to the creep damage because of the insufficient diffusion of vacancies required for the growth of cavities, while that lower than 10^{-4} s^{-1} corresponds to creep deformation [2,28].

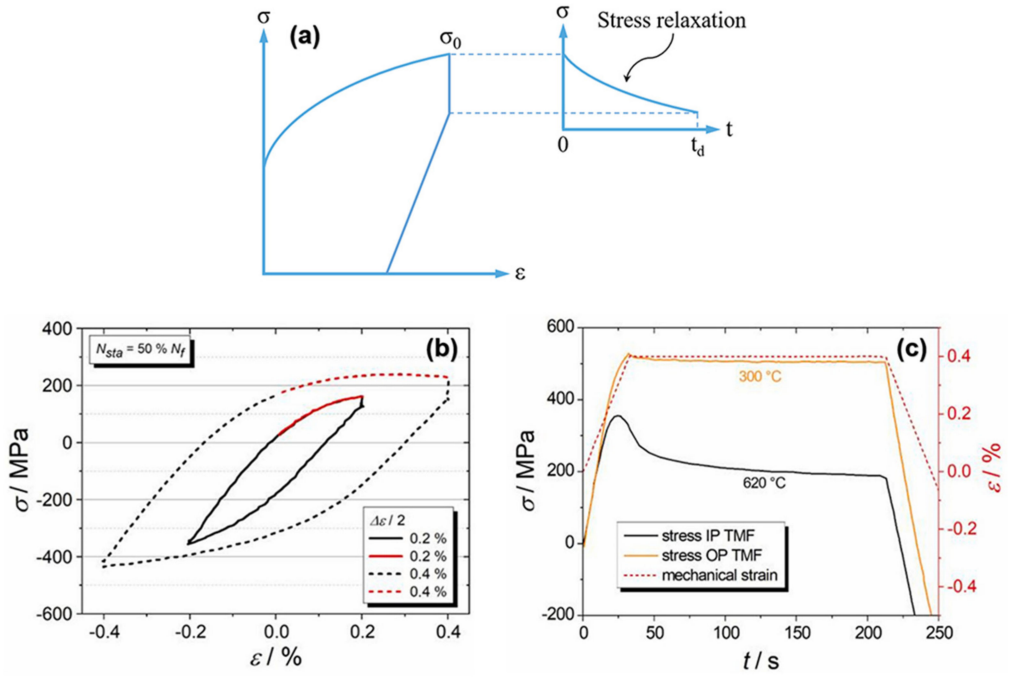


Figure 1. (**a**) Schematic illustration of the stress relaxation, and (**b**,**c**) stress relaxation in the stress-strain hysteresis loop at the half−life cycle and tensile strain dwell, respectively [9].

The stress relaxation behavior is affected by a series of factors, mainly including strain amplitude, dwell time, and temperature. Srinivasan et al. [15] studied the CFI behaviors of 316LN stainless steel at various strain amplitudes and found that the increased stress response with an increasing strain amplitude resulted in a higher tensile stress at the start of hold period, which provided a larger driving force for dislocation motion during the recovery process, consequently leading to an increase in the amount of stress relaxation [11]. The introduction of temperature cycling resulted in an increase of cyclic stress response; thus, its effect on the stress relaxation at half-life cycle was equivalent to the increase of strain amplitude. Meanwhile, it was found that the amount of stress relaxation at half-life cycle increased linearly with the increase of dwell time. Mechanisms of the phenomenon can be summarized as follows: (1) more significant creep damage caused by lower inelastic

strain rate [11,28], (2) more severe creep damage due to the longer duration for nucleation of cavities and grain boundary sliding [15], (3) greater viscoplastic deformation [24], and (4) annihilation of more dislocations caused by more sufficient thermal recovery process [19]. In addition, compared with CFI, the curve slope of stress relaxation at half-life cycle with dwell time under CTMF loading conditions was larger. However, Reddy et al. [2] found that the stress relaxation at half-life cycle decreased with the increase of dwell time and attributed it to the continuous hardening of matrix and the enhanced DSA effect. Moreover, with the increase of temperature, the thermal activation becomes stronger, which enhances the thermal recovery process and viscoplasticity of the material, thus increasing the stress relaxation at half-life cycle [29,30].

4. Damage Mechanisms under CTMF Loading Conditions

4.1. Thermomechanical Fatigue

Compared with IF, TMF loading condition is more complicated because of the phase angle between temperature cycling and mechanical loadings, in which in-phase (IP) and out-of-phase (OP) are most widely studied, as demonstrated in Figure 2. Since Young's modulus and strength values are temperature dependent, the TMF cycling yields a higher flow stress under compression coinciding with the low temperature regimes, which results in higher cyclic stress response than IF loading conditions. Moreover, under high temperature regimes the resistance of material to plastic deformation is attenuated, which leads to compressive mean stress under IP loading conditions and tensile mean stress under OP loading conditions [3,31]. Li et al. [32] presented that the cyclic stress response behavior of 316LN stainless steel was divided into three stages: cyclic hardening, cyclic softening, and rapid stress drop, which was closely related to the evolution of dislocation structures. During the initial cyclic hardening process, the dislocation density increased gradually, and the movement of dislocations was dominated by planar slip. Reddy et al. [2] attributed the cyclic hardening behavior to the interaction of (1) dislocation–dislocation, (2) dislocation–solute atom, and (3) dislocation–precipitation. During the cyclic softening process, thermal recovery promoted the annihilation of dislocation, thus decreasing the dislocation density and resulting in the evaluation of dislocation walls and cells. With the continuous softening, the development of substructures as well as the initiation and propagation of microcracks, coinciding with the rapid stress drop, indicated the formation of macroscopic cracks and fatigue failure of the material.

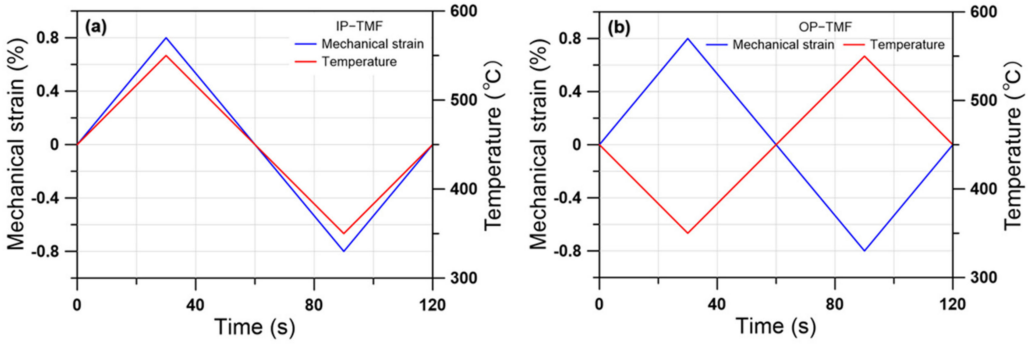


Figure 2. Schematic illustration of TMF tests under conditions of (**a**) IP and (**b**) OP, respectively.

There have been reported a large number of studies on TMF behaviors of austenitic stainless steel, including the effects of numerous factors, such as temperature, strain amplitude, strain rate, and nitrogen content [21,33,34]. Nagesha et al. [3] studied the TMF behaviors of 316LN stainless steel at various temperature ranges and found that the life behavior was related to whether the maximum testing temperature entered the creep temperature regimes. Specifically, in the sub-creep temperature range (Tmax < 600 °C), the fatigue life of OP-TMF loading conditions was lower than that of IP-TMF, which was attributed to earlier crack initiation and accelerated crack propagation caused by the tensile

mean stress and higher stress response [3,6]. However, in the creep temperature range (Tmax > 600 °C), IP-TMF loading conditions yielded lower fatigue life, which was attributed to more severe creep damage caused by the unidirectional accumulation of tensile grain boundary sliding as well as more severe oxidation damage due to the continuously opened crack tip during the high temperature regimes. Kuwabara et al. [21] studied the fatigue properties of 304 stainless steel and found that when the inelastic strain was larger than 0.7% the fatigue life of TMF loading conditions was longer than that of IF, while the opposite was true at lower strain amplitudes, which was attributed to more severe creep and oxidation damage aggravated by the temperature cycling. Reddy et al. [33] studied the TMF behaviors of 316LN stainless steel at different strain amplitudes and found that the fracture was dominated by transgranular mode under OP-TMF loading conditions and mixed mode under IP-TMF loading conditions, with the decrease of strain amplitude the proportion of intergranular cracks increasing. Neo et al. [34] proposed that the decrease of strain rate enhanced the oxidation and creep damage, which decreased the fatigue life, and the phenomenon was more obvious at low strain amplitudes. Nagesha et al. [3] found that compared with IF, more intergranular carbide precipitation occurred under TMF loading conditions, which was attributed to more nucleation sites at grain boundaries caused by the deformation during low temperature regimes. The accumulation of carbides at grain boundaries reduced the free energy between grains and resulted in a greater degree of lattice distortion and asymmetrical grain deformation, which promoted the occurrence of serrated grain boundaries, leading to more severe intergranular cracking. In addition, nitrogen can delay carbide precipitation and refine carbide precipitates to reduce local stress concentration, thus extending fatigue life [35].

4.2. Creep

As a complex process related to temperature, stress, and time, creep is an important damage mechanism which limits the service life of components under high temperature conditions. The creep curve describes the macroscopic creep process of materials through the relationship between creep strain and time, which can be divided into three stages, as demonstrated in Figure 3a. In addition, Figure 3b, originating from ref. [22], shows the evolution of creep strain with time under various stress loadings. Under lower stress level, the steady creep stage lasts for a long time. With the increase of stress, the duration of steady creep stage gradually decreases or even disappears. Therefore, under the actual service conditions, high-temperature materials are in the steady creep stage for quite a long period of time, and the evolution of microstructures and properties during the stage has a significant influence on the subsequent creep process and failure behavior.

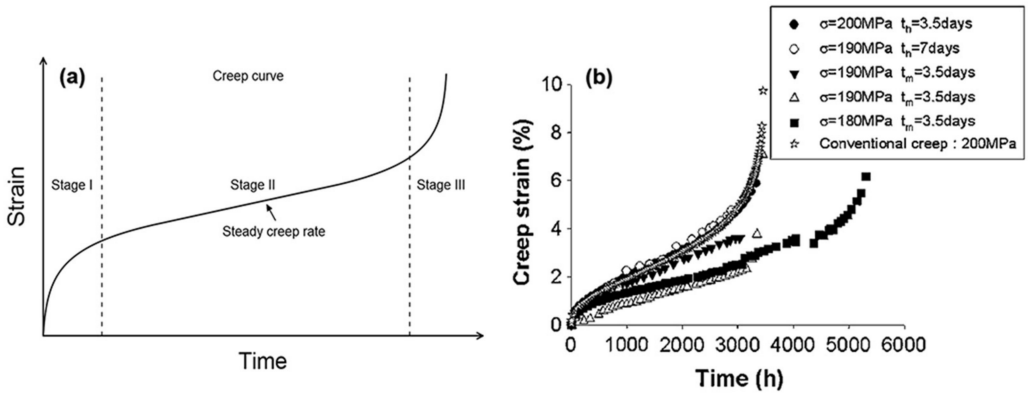


Figure 3. (**a**) Schematic illustration and (**b**) actual evolution of creep strain curve [22].

Under various stress levels and temperature conditions, the macroscopic creep deformation of materials is caused by the interaction of many complex processes, such as dislocation motion, atom diffusion, and grain boundary deformation. Scholars have divided creep mechanisms into four main types, namely dislocation slip, diffusional creep, creep cavity and grain boundary sliding. Numerous studies have shown that the dominant micro-mechanism of creep process is affected by a series of factors, including stress level, temperature, and nitrogen content. Creep process can change the diffusion gradient and distribution state of atoms, leading to their re-diffusion and redistribution, and some solute atoms preferentially undergo segregation at grain boundaries with higher distortion energy [16]. With the increase of temperature, the diffusion ability of solute atoms is enhanced, increasing the concentration of segregation gradually and then resulting in precipitation. Moreover, the redistribution of solute atoms greatly affects the motion and evolution of dislocations. Therefore, different temperature conditions can change the relative interaction between dislocation slip and diffusional creep. In addition, Kim et al. [16] found that with the decrease of stress level, the fatigue life increased and the proportion of intergranular cracks was larger. This was because when the creep cavity was the dominant mechanism, the increase of life led to more precipitation of carbides, which resulted in the preferential nucleation and growth of cavities at carbides. However, Ganesan et al. [1] found that with the decrease of stress level, the proportion of intergranular cracks firstly increased and then decreased. This was because when the grain boundary sliding was the dominant mechanism, more precipitation of carbides strengthened grain boundaries and hindered the grain boundary sliding, resulting in a decreased trend of the proportion of intergranular cracks. Therefore, the effect of stress level on creep behavior is closely related to the role of carbides in various creep mechanisms. In addition, as a strong solid solute strengthening element of austenitic stainless steel, N can improve creep strength and fracture toughness of materials [36–38]. Ganesan et al. [1] found that with the increase of N content from 0.07 wt.% to 0.22 wt.%, the creep fracture life could be extended by 10 times. It was because N reduced the layer fault energy to restrain the planar slip [39], and refined the carbides precipitated at grain boundaries, thus reducing the stress concentration to delay the nucleation of intergranular cracks.

Under the interaction of creep and fatigue, the intergranular damage caused by creep occurs in the matrix material, while the cracking damage caused by fatigue occurs on the surface of specimens. The interaction of these two damage mechanisms accelerates the crack initiation and promotes the crack propagation in the mixed mode, thus accelerating the failure of materials. At present, researchers have proposed numerous damage mechanisms of CFI, including: (1) intergranular crack propagation assisted by the connection of cavities [40], (2) larger plastic zone at crack tips caused by numerous cavities [34], and (3) wedge cracks at triple points of grain boundaries due to the grain boundary sliding [41]. Moreover, as the dominant creep mechanisms under CFI loading conditions, the coalescence of cavities and grain boundary sliding are related to the crack tip. Specifically, the coalescence of cavities is a process controlled by distance, which can occur only when the opening distance of the crack tip is larger than a certain critical value [42]. In addition, the grain boundary sliding is controlled by the stress field of the crack tip, and only when the stress of the crack tip is high enough can the lattice dislocations in slip bands be decomposed into mobile dislocations, thus leading to the occurrence of grain boundary sliding [43]. The growth of cavities can result in "R"-type intergranular cracks, while grain boundary sliding can lead to "W"-type wedge cracks at triple points of grain boundaries [44]. Figure 4a demonstrates the process of intergranular cracking dominated by two creep mechanisms, respectively. In addition, Figure 4b, originating from ref. [45], shows the morphologies of two types of cracks. Moreover, with the increase of stress level and the decrease of strain rate, creep damage caused by cavities and grain boundary sliding becomes more severe.

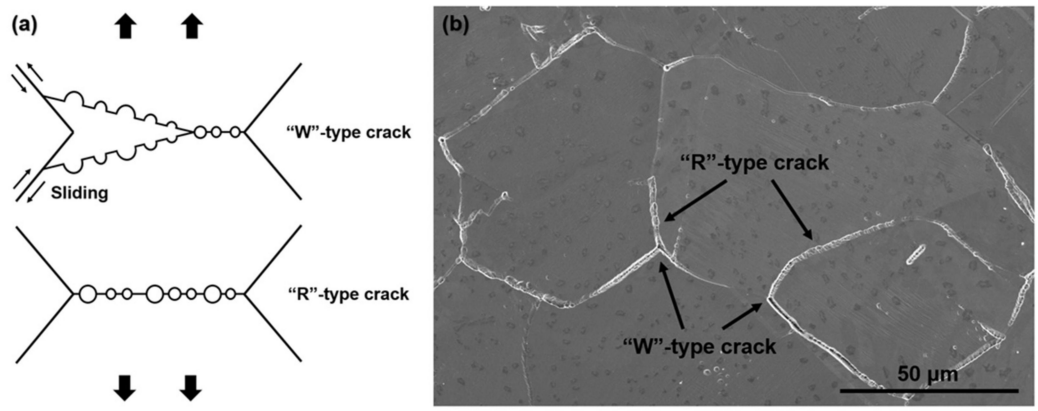


Figure 4. (**a**) Schematic illustrations and (**b**) actual morphologies of "W"-type and "R"-type cracks [45].

4.3. Oxidation

During the initial oxidation, the complete and stable oxide scale has not formed, in which the oxidation kinetics is closer to the linear law. After the stable oxide layer is formed, the diffusion of alloy elements controls the growth of the oxide scale, and the oxidation kinetics begins to follow a parabolic law. It is emphasized that the structural composition and distribution of oxides under cyclic loadings are significantly different from the oxidation behavior without mechanical loadings [46]. Karabela et al. [47] studied the influence of cyclic loadings on the oxygen diffusion in the oxidation process and found that the oxygen content in the oxide scale was higher under cyclic loadings, and the material was more easily oxidized under constant tensile loads, which was called stress-enhanced oxidation [48]. Weiss et al. [49] studied the interaction of oxidation and fatigue of 316 stainless steel and found that the surface oxide scale was a very thin layer of Cr2O3 without loads, while cyclic mechanical loading resulted in the formation of an external layer of Fe2O3 and an internal layer of FeCr2O4. In addition, under fatigue loading conditions oxides are preferentially formed at the surface slip bands [50,51]. With the continuous motion and accumulation of slip bands, defects will be formed on the sample surface, resulting in more oxygen penetrating into the matrix [31]. Therefore, oxidation has a great influence on the fatigue behaviors of metal materials. Neu et al. [34] found that, compared with the vacuum, the fatigue life under air environment was shortened to a large extent, which was attributed to the accelerated crack nucleation caused by the cracking of surface oxide scale. The cracking of oxide scale could be caused by the following factors [34,52], including: (1) mechanical strain on the specimen surface, (2) thermal stress caused by the deformation mismatch due to the various thermal expansion coefficients between the oxide scale and matrix material, (3) extra loads caused by the volume difference between the oxide layer and matrix material, (4) serious local deformation of oxide scale caused by the "intrusion" and "extrusion" on the specimen surface, (5) various creep behaviors between the oxide scale and matrix, and (6) the viscous slip of oxide scale on the substrate material. The author of the present paper [53] studied the oxidation behavior of 316LN stainless steel under IF and TMF loading conditions and found that under TMF loading conditions the temperature cycling resulted in the brittle cracking of oxide and debonding between oxide scale and substrate due to the thermal stress, which accelerated the initiation of microcracks, thus decreasing fatigue life. However, under the continuous high-temperature IF conditions, the dense and smooth oxide scale acted as a protective film for further oxygen penetration into the matrix without the development of deformation mismatch. Correspondingly, the effect of oxidation on the crack nucleation is marginal and the formation of surface intrusions and extrusions caused by the plastic deformation localization dominates the crack initiation, as shown in Figure 5, which originated from ref. [53]. Wu et al. [31] proposed that crack nucleation assisted by oxidation resulted in more short secondary cracks. However, there is no consensus on whether oxidation promotes or inhibits the crack

propagation. Some researchers found that the oxide scale could enhance the brittleness of the material near the crack tip. The formation and cracking of oxide layer at the crack tip continuously exposed the fresh matrix material to the oxygen environment, further accelerating oxygen ingression into the substrate, which led to more severe oxidation damage accompanied by crack propagation [54,55]. However, the opposite viewpoint was that the formation of oxide scale could lead to the passivation of the crack tip, and the highly branched crack tip caused by oxide cracking reduced the stress concentration at the crack tip, thus hindering the crack propagation [56]. In addition, in the theory of crack propagation assisted by oxidation, the oxygen diffusion process is classified as a short-range or long-range diffusion. The short-range diffusion is linked to the formation of grain boundary oxides, in which an incubation time is required. However, the long-range diffusion of oxygen lowers the grain boundary cohesive strength and results in grain boundary embrittlement, which does not require an incubation time [43]. The formation of intergranular oxides promotes the brittle cracking of grain boundaries, which accelerates the intergranular crack propagation, thus decreasing the fatigue life [47].

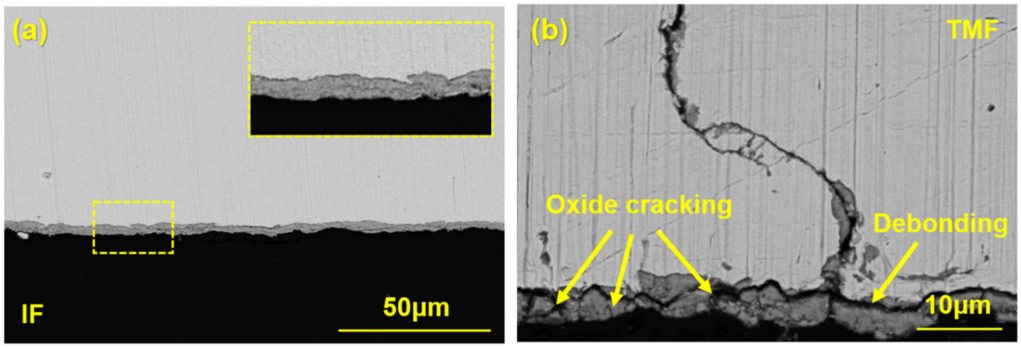


Figure 5. The morphologies of surface oxide scales under conditions of (**a**) IF and (**b**) TMF [53].

The interaction between oxidation and fatigue is affected by numerous factors, including strain amplitude, temperature, and strain-temperature phase angle [57–59]. Zhang et al. [60] studied the fatigue behaviors of 316LN stainless steel under high-pressure water environment and found that the decrease of strain amplitude resulted in more severe oxidation damage and fatigue life shortening, which was because oxidation was a time-dependent damage mechanism. At high strain amplitudes, due to the large plastic deformation and residual stress, the damage process was dominated by the mechanical loading, in addition to the weak oxidation caused by the short fatigue life, thus leading to the transgranular fracture mode. However, at low strain amplitudes, the enhanced oxidation damage due to the long time to fracture resulted in the fracture dominated by intergranular mode. Under TMF loading conditions, the introduction of temperature cycling leads to the thermal stress due to the deformation mismatch between oxide scale and substrate material [50], thus accelerating the crack initiation and propagation. Therefore, at low strain amplitudes, the fatigue life under TMF loading conditions is shorter than that under IF loading conditions, which is attributed to more severe oxidation damage. Generally, it is believed that, compared with OP-TMF, more severe oxidation damage under IP-TMF loading conditions accelerates crack nucleation. Some researchers presented that under IP-TMF loading conditions, the oxide scale formed during high temperature regimes became more brittle in the subsequent low temperature regimes. Meanwhile, the compressive stress imparted a more deleterious effect on the oxide scale [23,34], which promoted the oxide layer cracking [55]. Moreover, some other scholars proposed that the crack tip kept opened during high temperature regimes, resulting in more severe oxidation along grain boundaries [61].

4.4. Dynamic Strain Aging

Dynamic strain aging (DSA) is manifested in the form of the occurrence of stress serrations in the stress-strain hysteresis loop, inverse temperature dependence of the cyclic stress response, and inelastic strain at the half-life cycle [62]. In the DSA regime, mobile dislocations can be effectively pinned by obstacles and solute atom atmospheres during the process of movement, which requires a higher stress to maintain the progress of plastic deformation, followed by a rapid stress decrease after unpinning [63,64]. In addition, DSA enhances the degree of inhomogeneity of deformation by the solute locking of slow moving dislocations between planar slip bands, which inhibits the development of cross-slip, thus resulting in the cyclic hardening [61,65]. Nagesha et al. [3] found that dislocation structures changed from planar structures in the DSA regime to dislocation walls or cells in the no-DSA regime. Moreover, Li et al. [66] utilized the number of serrations to determine the action frequency of periodic dislocation pinning and unpinning processes, in order to achieve a quantitative evaluation of the DSA intensity.

As a time-dependent damage mechanism, DSA is affected by temperature, strain amplitude, and strain rate [67,68]. Solute atom atmospheres of various components are responsible for the pinning of mobile dislocations at different temperatures. At low temperatures (250 °C to 350 °C), the carbon-vacancy pairs and carbon atom clusters interacting with glide dislocations are reported to be responsible for DSA, while at high temperatures (400–650 °C), the chromium atoms that attain greater mobility contribute to DSA. Nagesha et al. [52] studied the TMF behaviors of 316LN stainless steel at various temperatures and found that the increasing maximum temperature of cycling enhanced the DSA intensity, which was because the higher density of vacancies caused by the stronger thermal vibration at high temperatures promoted the diffusion of solid solute atoms and pinning of dislocations. Meanwhile, with the increase of strain amplitude, the increased dislocation density and size of solute atom atmosphere decreased the mean free path of mobile dislocations, thus leading to the increased frequency of pinning. Pham et al. [69] studied the DSA behavior of 316L stainless steel at 300 °C and found that when mobile dislocations were kept for a sufficiently long time in dislocation forests, point defects could diffuse into mobile dislocations and then form atmospheres to strengthen locking mobile dislocations. Moreover, the slow motion of mobile dislocations at low strain rate resulted in long time of pinning, which enhanced the DSA intensity. The planar slip promoted by DSA impinging on grain boundaries can lead to heterogeneous plastic deformation, resulting in the serious local plastic deformation zone [16], which promotes the crack initiation. Meanwhile, DSA improves the strength of the material, which increases the cyclic stress response and leads to stronger stress concentration at the crack tip [16,52], thus accelerating crack propagation. Therefore, the occurrence of DSA generally results in the reduction of fatigue life of the material.

5. Fatigue Life Behavior under CTMF Loading Conditions

5.1. Effect of Strain Dwell Type on Life Behavior

According to the loading direction of strain dwell, the hold periods can be divided into three types, i.e., tensile strain dwell, compressive strain dwell, and tensile-compressive symmetrical strain dwell. Generally, compressive strain dwell results in higher cyclic stress response [15], and the reason is consistent with that of OP-TMF loading conditions. As for the influence of the type of strain dwell on the life behavior, numerous studies have shown that it is different for various materials. For the ferritic steels and super-alloy steels, such as René 95, compressive hold period is more detrimental to life behavior [70,71]. However, for the austenitic steels, tensile hold period results in shorter fatigue life [15,28]. Conway et al. [72] studied the CFI behaviors of 304 stainless steel with the asymmetric strain dwell and found that the fatigue life increased with the increase of compressive dwell time. Due to the low strength combined with the high brittleness of the internal grain boundaries of austenitic stainless steel [62], intergranular cracks occur more easily under

the action of creep damage. Therefore, more severe damage with tensile strain dwell is explained based on the micro-mechanisms of creep damage.

As for the mechanism of intergranular cavity, the diffusional growth of vacancies can occur only under the tensile loading, which is the prerequisite for the nucleation and growth of cavities [73]. Nevertheless, compressive strain dwell eliminates the cavities due to the sintering effect [15,42]. In addition, as for the mechanism of grain boundary sliding, the grain boundary sliding occurred during the tensile strain dwell is offset by the reverse one occurred during the compressive strain dwell, which results in the decrease of the amount of tensile grain boundary sliding [74]. Therefore, more severe creep damage only with the tensile strain dwell results in shorter fatigue life. In addition, the influence of hold period type on the fatigue life is related to the strain amplitude. Kuwabara et al. [21] found that at high strain amplitudes, the introduction of tensile strain dwell decreased fatigue life, while the compressive strain dwell had no significant effect on the life behavior. However, at low strain amplitudes, the introduction of tensile or compressive strain dwell decreased fatigue life obviously, which was due to the promoted grain boundary sliding process.

5.2. Effect of Dwell Time on Life Behavior

There are different opinions on whether the fatigue life decreases continuously or reaches the saturation with the increase of dwell time. Zhang et al. [11] found that when the dwell time was shorter than 1 min the strain dwell had a marginal effect on the fatigue life, while when the dwell time exceeded 1 min, the fatigue life decreased with the increase of dwell time linearly in the logarithmic coordinates. Numerous researchers [15,62] have found the continuous decrease of fatigue life with the increase of dwell time and attributed it to the increased proportion of intergranular cracks and accelerated crack propagation caused by more severe oxidation and creep damage [47,62]. However, Zhang et al. [11] also found that the fatigue life would no longer decrease and reach the saturation with the dwell time increasing to a certain critical value. Esztergar [75] proposed that the critical dwell time was particularly important, because the creep damage would no longer occur when the dwell time exceeded the critical value. In addition, Sauzay et al. [24] found that whether the decreased fatigue life reached the saturation was related to the strain amplitude. At high strain amplitudes, the fatigue life decreased continuously with the increase of dwell time, while at low strain amplitudes, the low stress level due to the long dwell time could not develop severe creep damage, which resulted in the saturation of decreased fatigue life. Levaillant et al. [76] attributed the phenomenon to the thermal aging effect. Min et al. [42] explained it based on the mechanism of creep cavity. Specifically, the enough free path on the grain boundaries was the prerequisite for the diffusional growth of cavities. Due to the incompatibility of polycrystalline materials, free path could not exist continuously, which led to the unsteady diffusional state of cavities. Therefore, the effect of hold period on the decrease of fatigue life reached the saturation gradually.

5.3. Effect of Temperature-Strain Phase Angle on Life Behavior

Similar to TMF loading conditions, according to the phase angle between the temperature cycling and mechanical loading, IP-CTMF and OP-CTMF are most widely studied. At present, it is generally believed that, compared with OP-CTMF loading conditions, the damage developed under IP-CTMF loading conditions is more severe. This can be mainly attributed to a series of factors as follows: (1) intergranular cracking promoted by the unidirectional accumulation of tensile grain boundary sliding [7,21], (2) growth and coalescence of intergranular cavities promoted by the temperature cycling [19], and (3) more severe oxidation damage caused by the continuously opened crack tips in the regimes of high temperature [8]. Therefore, under IP-CTMF loading conditions, the fracture is dominated by intergranular mode and the secondary cracks are longer [7,9]. The behavior characteristics of slow-fast loading conditions can be also explained based on these mechanisms [41]. Guth et al. [8] studied the influence of strain dwell on the TMF properties of nickel-based alloys and found that the crack initiation occurred earlier under

OP-CTMF loading conditions, while the accelerated crack propagation in the regimes of high temperature resulted in shorter fatigue life under IP-CTMF loading conditions.

However, there is no consensus on whether the introduction of temperature cycling decreases the fatigue life. It is generally believed that, compared with CFI loading conditions, the fatigue life under CTMF loading conditions is lower. Nevertheless, Takahashi et al. [28] found that sustained high temperature led to more severe oxidation damage, which resulted in shorter life under CFI loading conditions. In addition, the weld joints, inevitable in the construction of large-scale nuclear power structures, are characterized by heterogeneity in microstructures and mechanical properties. Meanwhile, due to the various coefficients of thermal expansion between the matrix material and weld metal, the temperature cycling under the actual serving conditions leads to geometrical discontinuities and local mismatch in strength between different constituents of the joints, which induces localized damage in low yielding zones and results in premature failure in the welded components [19,77].

6. Conclusions and Outlook

Research on the CTMF behaviors of austenitic stainless steel was reviewed to analyze and summarize the fatigue life behavior and associated damage mechanisms. Several conclusions were drawn as follows:

(1) TMF, creep, oxidation, and DSA are the main damage mechanisms of austenitic stainless steel for nuclear power pipelines under CTMF loading conditions. The coupled effects of various damage mechanisms can result in earlier crack initiation and accelerated crack propagation.

(2) Under CFI loading conditions, the creep damage mechanisms mainly include intergranular cavity and grain boundary sliding. In addition, compared with the amount of stress relaxation at the half-life cycle, the inelastic strain rate during the hold period is more suitable to characterize creep damage.

(3) By analyzing the influence of dwell type, dwell time and temperature-strain phase angle on the dominant failure mechanisms, the effects of various factors on the CTMF behaviors are summarized, which presents the theoretical support for predicting the CTMF life of nuclear-grade austenitic stainless steel under different loading conditions.

(4) The interaction between creep and fatigue accelerates damage accumulation under CFI loading conditions. Moreover, with the introduction of temperature cycling, i.e., CTMF loading conditions, nonconservative life prediction results are usually yielded based on the data generated by isothermal testing due to the synergistic interaction of more activated damage mechanisms.

It is of practical engineering significance to study the CTMF properties of austenitic stainless steel for nuclear power pipelines. Based on the detailed analysis and summary of the present work, the future research directions in the field are suggested as follows:

(1) Nuclear power pipelines are subjected to long-term loadings at low strain amplitudes under the actual service conditions. Therefore, CTMF tests with longer dwell time at low strain amplitudes need to be conducted. Moreover, thermal transients during the hold period should be considered to comprehensively analyze the interaction of creep, high cycle fatigue, and low cycle fatigue.

(2) Compared with CFI, CTMF loading configuration is more dangerous and closer to the real working conditions. Therefore, it is necessary to focus on the analysis of complex interaction of various damage mechanisms in order to explain failure modes and fatigue life behaviors of materials.

(3) Due to the introduction of temperature cycling, more activated damage mechanisms accelerate the failure of materials under CTMF loading conditions. Therefore, much more effort is needed to propose damage parameters based on the failure mechanisms, which consider the synergistic interaction of temperature cycling, loading, and oxidation, and develop life prediction models with clear physical meaning that are convenient for engineering application.

(4) At present, the creep-fatigue design curves commonly used in nuclear power design standards are determined based on the linear damage accumulation method. However, the damage accumulation rate under CFI loading conditions is much higher than the sum of damage accumulation rate under the individual action of fatigue and creep mechanisms. Therefore, a large number of CFI tests are required to evaluate the safety of existing design standards. It is necessary to develop a CTMF design curve more suitable for the actual service conditions.

Author Contributions: Conceptualization, J.Z.; methodology, J.Z.; validation, J.Z., F.Q., C.X.; formal analysis, J.Z.; investigation, J.Z.; writing—original draft preparation, J.Z.; writing—review and editing, J.Z.; visualization, F.Q. and C.X. All authors have read and agreed to the published version of the manuscript.

Funding: This research received no external funding.

Institutional Review Board Statement: The study did not require ethical approval.

Informed Consent Statement: The study did not involve humans.

Data Availability Statement: No new data were created or analyzed in this study. Data sharing is not applicable to this article.

Conflicts of Interest: The authors declare that they have no known competing financial interest or personal relationships that could have appeared to influence the work reported in this paper.

References

1. Ganesan, V.; Laha, K.; Mathew, M.D. Influence of nitrogen content on the evolution of creep damage in 316LN stainless steel. *Procedia Eng.* **2014**, *86*, 58–65. [CrossRef]
2. Reddy, G.V.P.; Parameswaran, P.; Sandhya, R.; Laha, K. Creep-fatigue interaction behavior of 316LN austenitic stainless steel with varying nitrogen content. *Mater. Des.* **2015**, *88*, 972–982. [CrossRef]
3. Nagesha, A.; Kannan, R.; Parameswaran, P.; Sandhya, R.; Rao, K.B.S.; Singh, V. A comparative study of isothermal and thermomechanical fatigue on type 316LN austenitic stainless steel. *Mater. Sci. Eng. A* **2010**, *527*, 5969–5975. [CrossRef]
4. Ellison, E.G.; Al-Zamily, A. Fracture and life prediction under thermal-mechanical strain cycling. *Fatigue Fract. Eng. Mater. Struct.* **1994**, *17*, 53–67. [CrossRef]
5. Bae, K.-H.; Kim, H.-H.; Lee, S.-B. Competing damage mechanisms in the thermo-mechanical fatigue of AISI 304L stainless steel. *Mater. Sci. Eng. A* **2011**, *529*, 417–424. [CrossRef]
6. Fournier, B.; Sauzay, M.; Caes, C.; Noblecourt, M.; Mottot, M.; Bougault, A.; Rabeau, V.; Pineau, A. Creep-fatigue-oxidation interactions in a 9Cr-1Mo martensitic steel. Part I: Effect of tensile holding period on fatigue lifetime. *Int. J. Fatigue* **2008**, *30*, 649–662. [CrossRef]
7. Guth, S.; Lang, K.-H. Influence of dwell times on microstructure, deformation and damage behavior of NiCr22Co12Mo9 under thermomechanical fatigue. *Mater. Sci. Eng. A* **2020**, *794*, 139970. [CrossRef]
8. Guth, S.; Petras, R.; Skorik, V.; Krumi, R.; Man, J.; Lang, K.H.; Polak, J. Influence of dwell times on the thermomechanical fatigue behavior of a directionally solidified Ni-base superalloy. *Int. J. Fatigue* **2015**, *80*, 426–433. [CrossRef]
9. Jurgens, M.; Sonntag, N.; Olbricht, J.; Fedelich, B.; Skrotzki, B. The effect of dwell time on the thermomechanical fatigue life performance of grade P92 steel at intermediate and low strain amplitudes. *Mater. Sci. Eng. A* **2021**, *805*, 140593. [CrossRef]
10. Bartoak, M.; Horvath, J.; Bartosak, M.; Rohlova, M. Life assessment of a low-alloy martensitic steel under isothermal low-cycle fatigue-creep and thermo-mechanical fatigue-creep loading conditions. *Int. J. Fatigue* **2020**, *145*, 106092. [CrossRef]
11. Zhang, X.; Tu, S.-T.; Xuan, F. Creep-fatigue endurance of 304 stainless steel. *Theor. Appl. Fract. Mech.* **2014**, *71*, 51–66. [CrossRef]
12. Hales, R. A quantitative metallographic assessment of structural degradation of type 316 stainless steel during creep-fatigue. *Fatigue Eng. Mater. Struct.* **1980**, *4*, 339–356. [CrossRef]
13. Zauter, R.; Christ, H.J.; Mughrabi, H. Mughrabi Some aspects of thermomechanical fatigue of AISI 304L stainless steel: Part I. creep-fatigue damage. *Metall. Mater. Trans. A* **1994**, *25*, 401–406. [CrossRef]
14. Alsmadi, Z.Y.; Alomari, A.; Kumar, N. Effect of hold time on high temperature creep-fatigue behavior of Fe-25Ni-20Cr (wt.%) austenitic stainless steel (Alloy 709). *Mater. Sci. Eng. A* **2020**, *771*, 138591. [CrossRef]
15. Srinivasan, V.S.; Nagesha, A.; Valsan, M.; Rao, K.B.S.; Mannan, S.L.; Sastry, D.H. Effect of hold-time on low cycle fatigue behavior of nitrogen bearing 316L stainless steel. *Int. J. Press. Vessel. Pip.* **1999**, *76*, 863–870. [CrossRef]
16. Kim, D.W.; Chang, J.-H.; Ryu, W.-S. Evaluation of the creep-fatigue damage mechanism of type 316L and type 316LN stainless steel. *Int. J. Press. Vessel. Pip.* **2008**, *85*, 378–384. [CrossRef]

17. Sarkar, A.; Okazaki, M.; Nagesha, A. Mechanisms of failure under low cycle fatigue, high cycle fatigue and creep interactions in combined cycling in a type 316LN stainless steel. *Mater. Sci. Eng. A* **2017**, *683*, 24–36. [CrossRef]
18. Nagesha, A.; Valsan, M.; Kannan, R.; Rao, K.B.S.; Bauer, V.; Christ, H.-J.; Singh, V. Thermomechanical fatigue evaluation and life prediction of 316L(N) stainless steel. *Int. J. Fatigue* **2009**, *31*, 636–643. [CrossRef]
19. Kumar, T.S.; Nagesha, A.; Kannan, R. Thermal cycling effects on the creep-fatigue interaction in type 316LN austenitic stainless steel weld joint. *Int. J. Press. Vessel. Pip.* **2019**, *178*, 104009. [CrossRef]
20. Sarkar, A.; Dash, M.K.; Nagesha, A.; Dasgupta, A.R. EBSD based studies on various modes of cyclic deformation at 923K in a type 316LN stainless steel. *Mater. Sci. Eng. A* **2018**, *723*, 229–237. [CrossRef]
21. Kuwabara, K.; Nitta, A. Thermal-mechanical low-cycle fatigue under creep-fatigue interaction on type 304 stainless steel. *Fatigue Eng. Mater. Struct.* **1979**, *2*, 293–304. [CrossRef]
22. Fournier, B.; Sauzay, M.; Caes, C.; Noblecourt, M.; Pineau, A. Creep-fatigue interactions in a 9Cr-1Mo martensitic steel. Part I: Mechanical test results. *Metall. Mater. Trans. A* **2009**, *40*, 321–329. [CrossRef]
23. Goswami, T.; Hanninen, H. Dwell effects on high temperature fatigue damage mechanisms Part II. *Mater. Des.* **2001**, *22*, 217–236. [CrossRef]
24. Sauzay, M.; Mottot, M.; Allais, L.; Noblecourt, M.; Monnet, I. Creep-fatigue behavior of an AISI stainless steel at 550 °C. *Nucl. Eng.* **2004**, *232*, 219–236. [CrossRef]
25. Wood, D.S.; Banks, P. The creep/fatigue behavior of type 316 steel under reverse bending conditions. *Fatigue Fract. Eng. Mater. Struct.* **1990**, *13*, 551–561. [CrossRef]
26. Wang, J.; Li, N.; Anderoglu, O.; Zhang, X.; Misra, A.; Huang, J.Y.; Hirth, J.P. Detwinning mechanisms for growth twins in face-centered cubic metals. *Acta Mater.* **2010**, *58*, 2262–2270. [CrossRef]
27. Dewa, R.T.; Park, J.H.; Kim, S.J.; Sang, L. High-temperature creep-fatigue behavior of alloy 617. *Metals* **2018**, *8*, 103. [CrossRef]
28. Takahashi, Y.; Shibamoto, H.; Inoue, K. Study on creep-fatigue life prediction methods for low-carbon nitrogen-controlled 316 stainless steel (316FR). *Nucl. Eng. Des.* **2008**, *238*, 322–335. [CrossRef]
29. Li, B.; Zheng, Y.; Shi, S.; Chen, X. Microcrack nucleation and early crack growth of a nuclear grade nitrogen alloyed austenitic stainless steel X2CrNiMo18.12 under thermomechanical fatigue loading. *Int. J. Press. Vessel. Pip.* **2019**, *172*, 188–198. [CrossRef]
30. Holmstrom, S.; Pohja, R.; Nurmela, A.; Moilanen, P.; Auerkari, P. Creep and creep-fatigue behavior of 316 stainless steel. *Procedia Eng.* **2013**, *55*, 160–164. [CrossRef]
31. Wu, H.; Yang, B.; Wang, S.; Zhang, M. Effect of oxidation behavior on the corrosion fatigue crack initiation and propagation of 316LN austenitic stainless steel in high temperature water. *Mater. Sci. Eng. A* **2015**, *633*, 176–183. [CrossRef]
32. Li, B.; Zheng, Y.; Shi, S.; Zhang, Z.; Chen, X. Cyclic deformation and cracking behavior of 316LN stainless steel under thermomechanical and isothermal fatigue loadings. *Mater. Sci. Eng. A* **2020**, *773*, 138866. [CrossRef]
33. Reddy, G.V.P.; Nagesha, A.; Kannan, R.; Sandhya, R.; Laha, K. Thermomechanical fatigue behavior of nitrogen enhanced 316LN stainless steel: Effect of cyclic strain. *Int. J. Fatigue* **2017**, *103*, 176–184. [CrossRef]
34. Neu, R.W.; Sehitoglu, H. Thermomechanical fatigue, oxidation and creep: Part I. damage mechanisms. *Metall. Trans. A* **1989**, *20*, 1755–1767.
35. Kim, D.W.; Kim, W.G.; Rye, W.-S. Role of dynamic strain aging on low cycle fatigue and crack propagation of type 316LN stainless steel. *Int. J. Fatigue* **2003**, *25*, 1203–1207. [CrossRef]
36. Ganesan, V.; Mathew, M.D.; Parameswaran, P.; Laha, K. Effect of nitrogen on evolution of dislocation substructure in 316LN SS during creep. *Procedia Eng.* **2013**, *55*, 36–40. [CrossRef]
37. Reddy, G.V.P.; Kannan, R.; Mariappan, K.; Sandhya, R.; Sankaran, S.; Rao, K.B.S. Effect of strain rate on low cycle fatigue of 316LN stainless steel with varying nitrogen content: Part-I cyclic deformation behavior. *Int. J. Fatigue* **2015**, *81*, 299–308. [CrossRef]
38. Reddy, G.V.P.; Sandhya, R.; Rao, K.B.S.; Sankaran, S. Influence of nitrogen alloying on dynamic strain ageing regimes in low cycle fatigue of AISI 316LN stainless steel. *Procedia Eng.* **2010**, *2*, 2181–2188. [CrossRef]
39. Shankar, P.; Shaikh, H.; Sivakumar, S. Effect of thermal aging on the room temperature tensile properties of AISI type 316LN stainless steel. *J. Nucl. Mater.* **1999**, *264*, 29–34. [CrossRef]
40. Majumdar, S. Relationship of creep, creep-fatigue and cavitation damage in type 304 austenitic stainless steel. *J. Eng. Mater. Technol.* **1989**, *111*, 123–131. [CrossRef]
41. Baik, S.; Raj, R. Mechanisms of creep-fatigue interaction. *Metall. Trans. A* **1982**, *13*, 1215–1221. [CrossRef]
42. Min, B.K.; Raj, R. Hold-time effects in high temperature fatigue. *Acta Metall.* **1978**, *26*, 1007–1022. [CrossRef]
43. Maciejewski, K.; Dahal, J.; Sun, Y. Creep-environment interactions in dwell-fatigue crack growth of nickel based superalloys. *Metall. Mater. Trans. A* **2014**, *45*, 2508–2521. [CrossRef]
44. Rodriguez, P.; Rao, K.B.S. Nucleation and growth of cracks and cavities under creep-fatigue interaction. *Prog. Mater. Sci.* **1993**, *37*, 403–480. [CrossRef]
45. Zhao, J.; Li, B.; Zheng, Y.; Mohammad, A.; Chen, X. Cyclic deformation behavior and failure mechanism of 316LN stainless steel under creep-fatigue loading at 550 °C. *J. Mater. Eng. Perform.* **2022**, *4*, 8314–8326. [CrossRef]
46. Chen, J.; Nurrochman, A.; Hong, J.-D. Comparison of oxide layers formed on the low-cycle fatigue crack surfaces of Alloy 690 and 316 SS tested in a simulated PWR environment. *Nucl. Eng. Technol.* **2019**, *51*, 479–489. [CrossRef]

47. Karabela, A.; Zhao, L.; Lin, B.; Tong, J.; Hardy, M.C. Oxygen diffusion and crack growth for a nickel-based superalloy under fatigue-oxidation conditions. *Mater. Sci. Eng.A* **2013**, *567*, 46–57. [CrossRef]
48. Evans, H.E. Stress effects in high temperature oxidation of metals. *Int. Mater. Rev.* **1995**, *40*, 1–40. [CrossRef]
49. Weiss, J.; Pineau, A. Fatigue and creep-fatigue damage of austenitic stainless steel under multiaxial loading. *Metall. Trans. A* **1993**, *24*, 2247–2261. [CrossRef]
50. Li, B.; Zheng, Y.; Li, Q.; Liu, C.; Chen, X. Thermomechanical fatigue properties and microstructural damage of nitrogen alloyed 316LN stainless steel. *Int. J. Fatigue* **2020**, *138*, 105704. [CrossRef]
51. Gao, J.; Tan, J.; Wu, X.; Xia, S. Effect of grain boundary engineering on corrosion fatigue behavior of 316LN stainless steel in borated and lithiated high-temperature water. *Corros. Sci.* **2019**, *152*, 190–201. [CrossRef]
52. Nagesha, A.; Kannan, R.; Srinivasan, V.S. Dynamic strain aging and oxidation effects on the thermomechanical fatigue deformation of reduced activation ferritic-martensitic steel. *Metall. Mater. Trans. A* **2016**, *47*, 47–1127. [CrossRef]
53. Zhao, J.; Li, B.; Chen, G.; Takamoto, I.; Chen, X. Effect of dwell time on the isothermal and thermomechanical fatigue behavior of 316LN stainless steel. *Int. J. Fatigue* **2022**, *162*, 106989. [CrossRef]
54. Bartosák, M.; Horváth, J.; Spaniel, M. Multiaxial low-cycle thermal-mechanical fatigue of a low-alloy martensitic steel: Cyclic mechanical behavior, damage mechanisms and life prediction. *Int. J. Fatigue* **2021**, *151*, 106383. [CrossRef]
55. Warner, H.; Calmunger, M.; Chai, G. Thermomechanical fatigue behavior of aged heat resistant austenitic alloys. *Int. J. Fatigue* **2019**, *127*, 509–521. [CrossRef]
56. Chang, L.; Li, X.; Wen, J.; Zhou, B.; Zhou, C. Thermal-mechanical fatigue behavior and life prediction of P92 steel, including average temperature and dwell effects. *J. Mater. Res. Technol.* **2020**, *9*, 819–837. [CrossRef]
57. Christ, H.-J. Effect of environment on thermomechanical fatigue life. *Mater. Sci. Eng. A* **2007**, *468–470*, 98–108. [CrossRef]
58. Petrás, R.; Skorik, V.; Polak, J. Thermomechanical fatigue and damage mechanisms in Sanicro-25 steel. *Mater. Sci. Eng. A* **2016**, *650*, 52–62. [CrossRef]
59. Petrás, R.; Polák, J. Damage mechansim in austenitic steel during high temperature cyclic loading with dwells. *Int. J. Fatigue* **2018**, *113*, 335–344. [CrossRef]
60. Zhang, Z.; Tan, J.; Wu, X.; Han, E.; Ke, W. Synergistic effect of mechanical and environmental damages of 316LN stainless steel under different fatigue strain amplitudes in high-temperature pressurized water. *Mater. Sci. Eng. A* **2019**, *743*, 243–250. [CrossRef]
61. Calmunger, M.; Chai, G.; Johansson, S. Creep and fatigue interaction behavior in Sanicro 25 heat resistant austenitic stainless steel. *Trans. Indian Inst. Met.* **2016**, *69*, 337–342. [CrossRef]
62. Srinivasan, V.S.; Valsan, M.; Rao, K.; Mannan, S.L.; Raj, B. Low cycle fatigue and creep-fatigue interaction behavior of 316LN stainless steel and life prediction by artificial neural network approach. *Int. J. Fatigue* **2003**, *25*, 1327–1338. [CrossRef]
63. Zhou, H.; Bai, F.; Yang, L.; Wei, H.; Chen, Y. Mechanism of dynamic strain aging in a niobium-stabilized austenitic stainless steel. *Metall. Mater. Trans. A* **2018**, *49*, 1202–1210. [CrossRef]
64. Zhou, H.; He, Y.; Cui, M.; Cen, Y.; Jiang, J. Dependence of dynamic strain aging on strain amplitudes during the low-cycle fatigue of TP347H austenitic stainless steel at 550 °C. *Int. J. Fatigue* **2013**, *56*, 1–7. [CrossRef]
65. Li, H.; Jing, H.; Xu, L.; Zhao, L.; Han, Y.; Tang, Z.; Xiao, B.; Zhang, Y. Life, dislocation evolution and fracture mechanism of a 41Fe-25.5Ni-23.5Cr alloy during low cycle fatigue at 700 °C. *Int. J. Fatigue* **2018**, *119*, 20–33. [CrossRef]
66. Li, B.; Zheng, Y.; Zhao, J.; Shi, S.; Zhang, Z.; Chen, X. Cyclic deformation behavior and dynamic strain aging of 316LN stainless steel under low cycle fatigue loadings at 550 °C. *Mater. Sci. Eng. A* **2021**, *818*, 141411. [CrossRef]
67. Sarkar, A.; Nagesha, A.; Parameswaran, P.; Murugesan, S.; Sandhya, R.; Laha, K. Insights into dynamic strain aging under cyclic creep with reference to strain burst: Some new observations and mechanisms. Part-1: Mechanistic aspects. *Mater. Sci. Eng. A* **2016**, *660*, 213–224. [CrossRef]
68. Nagesha, A.; Kannan, R.; Sastry, G.V.S.; Sandhya, R.; Singh, V.; Rao, K.B.S.; Mathew, M.D. Isothermal and thermomechanical fatigue studies on a modified 9Cr-1Mo ferritic martensitic steel. *Mater. Sci. Eng. A* **2012**, *554*, 95–104. [CrossRef]
69. Pham, M.S.; Holdsworth, S.R. Dynamic strain ageing of AISI 316L during cyclic loading at 300°C: Mechanism, evolution and its effects. *Mater. Sci. Eng. A* **2012**, *556*, 122–133. [CrossRef]
70. Fournier, B.; Sauzay, M.; Caes, C.; Noblecourt, M.; Mottot, M. Bougault, A. Rabeau, V.; Pineau, A. Creep-fatigue-oxidation interactions in a 9Cr-1Mo martensitic steel. Part II: Effect of compressive holding period on fatigue lifetime. *Int. J. Fatigue* **2008**, *30*, 663–676. [CrossRef]
71. Shankar, V.; Valsan, M.; Rao, K.B.S.; Kannan, R.; Mannan, S.L.; Pathak, S.D. Low cycle fatigue behavior and microstructural evolution of modified 9Cr-1Mo ferritic steel. *Mater. Sci. Eng. A* **2006**, *437*, 413–422. [CrossRef]
72. Conway, J.B.; Stentz, R.H.; Berling, J.T. *Fatigue, Tensile and Relaxation Behavior of Stainless Steel*; Mar-Test: Cincinnati, OH, USA, 1975.
73. Nam, S.W. Assessment of damage and life prediction of austenitic stainless steel under high temperature creep-fatigue interaction condition. *Mater. Sci. Eng. A* **2002**, *322*, 64–72. [CrossRef]
74. Koterazawa, R.; Nosho, T. Creep-fatigue crack growth and fractography of a type 304 stainless steel at elevated temperature. *Fatigue Fract. Eng. Mater. Struct.* **1991**, *14*, 1–9. [CrossRef]
75. Esztergar, E.P. *Creep-Fatigue Interaction and Cumulative Damage Evolutions for Type 304 Stainless Steel*; National Laboratory: Oak Ridge, TN, USA, 1972.

76. Levaillant, C.; Grattier, J.; Mottot, M.; Pineau, A. Creep and creep-fatigue intergranular damage in austenitic stainless steels: Discussion of the creep-dominated regime. *J. ASTM Int.* **1988**, *942*, 414–437.
77. Kumar, T.S.; Nagesha, A.; Kumar, J.G.; Kannan, R. Influence of thermal aging on tensile and low cycle fatigue behavior of type 316LN austenitic stainless steel weld joint. *Metall. Trans. A* **2018**, *49*, 3257–3273. [CrossRef]

Disclaimer/Publisher's Note: The statements, opinions and data contained in all publications are solely those of the individual author(s) and contributor(s) and not of MDPI and/or the editor(s). MDPI and/or the editor(s) disclaim responsibility for any injury to people or property resulting from any ideas, methods, instructions or products referred to in the content.